# Photomemristive Heterostructures based on Two-Dimensional Crystals

**Gennady N. Panin[1, 2, *], Olesya O. Kapitanova[3]**

[1]*Department of Physics, Nano-Information Technology Academy, Dongguk University, Seoul, 04620, Republic of Korea*
[2]*Institute for Microelectronics Technology and High Purity Materials, Russian Academy of Sciences, Chernogolovka, Moscow Distr., 142432 Russia*
[3]*Department of Chemistry, Moscow State University, Moscow, 119991 Russia*

*Corresponding author: Tel: (+82) 02 2290 1360; E-mail: g_panin@dgu.edu, panin@iptm.ru

## Abstract

The unique electronic and optical properties of recently discovered two-dimensional (2D) crystals, such as graphene, graphene oxide, molybdenum disulphide etc., demonstrate their enormous potential in creating ultrahigh density electronics for image recognition systems and information storage. Synapse-like memristive heterostructures are considered as a new type of electronic switches with extremely low power consumption and footprint that can be used to overcome the limit of current CMOS technology. Memristors with a floating photogate, called photomemristors, based on graphene and $MoS_2$, are considered. Photocatalytic oxidation of graphene is considered as an effective method for creating memristive heterostructures with photoresistive switching for non-volatile electronic memory of ultrahigh density for the formation of self-assembled nanoscale memristive elements interfacing with neural networks. 2D photomemristors with a floating photogate exhibit multiple states that can be monitored over a wide range of electromagnetic radiation and can be used in neurohybrid systems for image processing and pattern recognition, as well as for selective manipulation of neurons by light. Copyright © VBRI Press.

**Keywords:** 2D crystals, memristor, photomemristive switching, floating photogate, neurohybrid systems.

## Introduction

High and ever-growing demands for working with big data, in particular unstructured data strongly motivate the creation of new brain-like machines for neuromorphic computations and neural networks that can overcome the limits of modern digital electronics.

Von Neumann architecture of digital computers based on silicon CIMOS technology was designed to solve clearly defined problems with well-defined data and now is ineffective for processing complex, unstructured and noisy data: a pattern, sound, motion and image recognition. The separation between the memory and the processor in the digital computer (**Fig. 1a**) causes traffic issues, which limits the efficiency of power consumption and performance. For example, modeling a neural network with 1% neurons of human cord using a Fujitsu "K Computer" supercomputer with digital processing of information (10 petaflops ($10^{16}$ billion operations per second), 1 petabyte RAM) required ~ 10 MW of power. To model the work of the human brain during 1 second, the supercomputer needed ~ 40 minutes. To model mouse cortex with $10^4$ neurons and $10^{10}$ synapses, a supercomputer "Blue Gene" was used, providing $10^9$ transistors (1 laptop per neuron) and consuming about one hundred kilowatts of power. Limiting the scaling of modern digital electronics based

on silicon CMOS technology has become a serious problem, which leads to chip heating and increased power consumption. Recently, Samsung demonstrated 7 nm FinFET, which is very close to the low power technology limit (5 nm) [**1**], which indicates the urgency of developing new materials and new approaches to calculation.
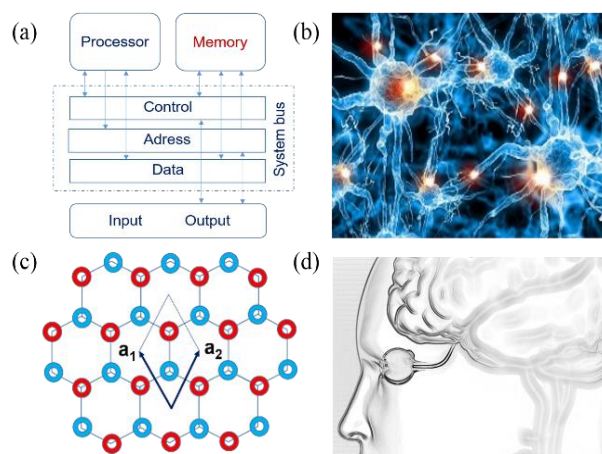


**Fig. 1.** (a) Von Neumann architecture of a digital computer, (b) Neural network, (c) The honeycomb lattice of graphene. The unit cell defined by vectors $a_1$ and $a_2$ containing the two atoms belonging to equivalent sublattices, (d) Retinal prostheses based on graphene [**10**].

Memristive electronic systems, similar to biological synapses in neural networks, are a new type of electronic logic switches and memory with extremely low energy consumption and footprint. These new electronic components can solve the problem of physical and technological limitations of modern CMOS technology and can become an elementary base for creating artificial intelligence. The definition of the memristor as a nonlinear resistive element was introduced by Leo Chua in 1971 to describe the missing fourth base element of the electrical circuit [**2**]. The memristor, along with other known circuit elements, such as a capacitor, a resistor and an inductor, could describe nonlinear effects in solid state electronics that were already well known. In 1922, Oleg Losev observed a new phenomenon of negative differential resistance in a two-electrode point device— a cristadyne [**3, 4**] - which was then used to generate and detect a signal for radio broadcasting around the world. Losev's cristadyne allowed to work at frequencies up to 100 MHz, at that time not conceivable and not understandable for applications. In 1957, Leo Esaki demonstrated independently a similar nonlinear device—a tunnel diode—and in 1973 received for the discovery of this effect the Nobel Prize in Physics.

Interest in the nonlinear two-electrode memristive device increased sharply in 2008, when the memristor was detected experimentally [**5**]. This device consisted of two nanoscale regions, doped and undoped, the relative displacement of which controlled the on and off states. The first matrix of memristors was made on the basis of $TiO_2$ on a CMOS chip in the HP laboratory in 2012. A memristor with two platinum electrodes was a nonlinear dynamic structure whose resistance depended on the electric field and the current flow. This nonlinear device made it possible to form nonvolatile states that allow storing information with the power supply off, had the ability to obtain ultrahigh recording density, low switching energy, high operating speed, long storage time and the possibility of multilevel recording using discrete or continuous states.

A number of complex computational problems for image processing and pattern recognition can be effectively solve using a nonlinear dynamic approach. For example, a Toshiba Smart Photo Sensor with a universal chip based on a cellular neural network (CNN) is capable of processing images, similar to the human brain, which allows to calculate the elementary problems of image recognition within nanoseconds. Memristors, which are similar to synapses in biological neural networks, can become an elemental base for creating high-performance intelligent machines and computers with a neuromorphic architecture similar to the brain. It is known that the human brain, containing $10^{11}$ neurons and $10^{15}$ synapses (**Fig. 1b**), processes analog information and consumes only about 20 Watts. Brain-inspired computing requires massively parallel operation with high random connectivity of neurons, processing signal and memory states, and storing altered memory states in synapses. Analog processing of information is effective for the solution and processing of unstructured sensory data, such as image, video, sound, movement, etc.

Brain-like devices might have architecture similar to the living nervous system. The cerebral cortex has ~0.15 quadrillion ($10^{15}$) of synapses or a trillion of synapses/per $cm^3$ ($10^{12}/cm^3$). For comparison, a 7 nm FinFET Samsung chip provides 40 billion switches ($4 \times 10^{10}/cm^2$). The brain contains of ~150,000-180,000 km of nerve fibers at age 20, connecting all these neuronal elements. Each neuron is able to contact any other neuron with no more than six connections - "six degrees of separation." About 85,000 neurons die per day or about 1 neuron per second. Thus, understanding the mechanisms of self-organization and self-healing of neuromorphic systems would allow the creation of electronic networks, similar to living neural ones.

The unique electronic and optical properties of newly discovered atomic two-dimensional (2D) crystals, such as graphene, graphene oxide, molybdenum disulfide and so on demonstrate a huge potential for designing ultrahigh density nano- and bioelectronics for innovative information systems. Graphene is a crystalline two-dimensional (2D) layer of carbon with the thickness of one atom. The unit cell in the honeycomb lattice of graphene defined by vectors $a_1$ and $a_2$ (**Fig. 1c**) containing the two atoms belonging to equivalent sublattices. A huge interest in this material appeared in 2004 after the joint publication of researchers from IMT RAS and Manchester University on the effect of an electric field in atomic-thin carbon films [**6**]. In 2010, Andrei Geim and Konstantin Novoselov were awarded the Nobel Prize in Physics for "pioneering experiments with 2D graphene material". Graphene consists of two symmetric carbon sublattices that form the Dirac cone of the linear energy dispersion of the electrons, which are called Dirac fermions. The peculiarity of these particles is that they are massless and behave like photons. In consequence, graphene demonstrates magical properties. Graphene transparent (97.7%), resistant to an extremely high current density (one million times higher than that of copper), has the highest electron mobility of known materials (~$10^6$ $cm^2$ $V^{-1}$ $s^{-1}$, three orders of magnitude higher than in silicon) and a very high thermal conductivity (K > $5 \times 10^3$ W/ (m × K)), which is higher than that of a diamond. Graphene is a well stretchable (25%) material with a unique mechanical strength E > $10^{12}$ Pa (six times higher than steel). In addition, graphene shows very good biocompatibility. Retinal neurons are able to survive and grow neurites on graphene [**7**]. Moreover, graphene FET arrays can record action potentials from cells [**8**]. This makes it possible to produce an artificial retinal display where, after processing the information, acquired by the camera that is mounted on the glasses, it is transferred to a retinal graphene implant that stimulates nerve cells to transmit a signal to the brain [**9**]. Recently, at the Mobile World Congress 2017 in Barcelona, the Catalan Institute of Nanoscience and Nanotechnology (ICN2)

demonstrated retinal prostheses based on graphene (**Fig. 1d**) [**10**]. These devices take advantage of the electrical properties, flexibility and biocompatibility of graphene. The device could allow partially recovering the vision to people who have lost the functionality of the photosensitive cells of the retina. Sensory evoked responses of built-in GFET were also demonstrated [**11**]. Recordings were obtained from the primary visual and primary auditory cortices of rats during sensory stimulation. An On–Off visually evoked response occurred 40 ms after the stimulus. The signal shows a main component with a frequency around 20 Hz with maximum amplitude of 250 μV and that lasts 70 ms.

In this paper we focus on 2D photoresistive memory based on molybdenum and graphene/graphene oxide (G/GO), which is biocompatible and allows the use of a neuromorphic architecture for analog computation and self-assembly technology. Photocatalytic oxidation of graphene is considered as an effective method of manufacturing 2D memristors with photoresistive switching for nonvolatile memory of ultrahigh capacity. A new type of multifunctional memristor with a photogate, controlled electrically and optically over a wide range of wavelengths, can be used for image processing, pattern recognition, recognition of sounds, movements and speech needed to create artificial intelligence, as well as for interaction of electronic networks and neurons.

## Experimental

### Material synthesis / device fabrications

Graphene was synthesized on a copper foil 25 μm thick at 1020°C by the method of chemical vapor deposition using a mixture of methane and hydrogen [**12**]. The grown graphene was transferred to a $SiO_2/Si$ substrate using PMMA. ZnO nanoparticles (NP) were obtained by thermal decomposition of zinc salts [**12**]. A 0.005 M solution of ethanol zinc acetate dihydrate was applied by a spin coating to a graphene/$SiO_2$/Si substrate at 1000 rpm and then annealed at 350°C for 40 minutes to form a layer of nanoparticles on graphene. A 2–3-layer graphene coated with particles was irradiated in a moist air stream at room temperature or above (80°C) using a quartz UV lamp with a light flux of 0.03 J $min^{-1} \times cm^2$. Light with a wavelength exceeding 365 nm was filtered. The time of ultraviolet irradiation ranged from 5 to 90 min. After ultraviolet treatment, the ZnO nanoparticles were dissolved in dilute 0.1 M HCl, the graphene substrate was washed with deionized water and dried in nitrogen. $MoS_2$ nanocrystals were grown using hydrothermal method [**13**]. The dispersion of $MoS_2$ in isopropyl alcohol was covered with a spin coating on a Si/$SiO_2$ substrate and annealed at 200°C for 15 minutes. Finally, the Au electrodes were made using photolithography and the lift-off process. After that, the samples were annealed in a 200 sccm flow ($H_2/N_2$ = 2: 3) at 450 °C for 15 minutes.

### Characterizations / measurements

The sample structure was analyzed by high-resolution transmission electron microscopy and micro-Raman spectrometry at room temperature. The morphology and chemical composition of the nanostructures were investigated using field emission scanning electron microscopy. Current-voltage characteristics of the fabricated structures were examined at room temperature in the dark and under white light using a Keithley 4200 SCS semiconductor analyzer with LabVIEW software in sweeping mode.

## Results and discussion

### Memristor based on graphene/graphene oxide

In 2010, researchers from IMT RAS and Dongguk University demonstrated a graphene/graphene oxide (G/GO) memristor that switched at 0.7 V and 1 nA, with an on/off ratio of about $10^3$ [**14-16**]. The electron beam-induced current method made it possible to reveal, with a high spatial resolution, the formation of randomly distributed current filaments (**Fig. 2**) and to study the switching mechanism in this device like a synapse. The resistance of this device varied nonlinearly in the electric field, and the values of high and low resistance were nonvolatile. The study of mechanisms of resistive switching in G/GO showed that the migration of oxygen-containing groups plays an important role [**14-18**]. One $sp^3$ carbon-oxygen or carbon-hydroxyl bond on $10^6$ $sp^2$ bonds reduced conductivity in carbon nanomaterials by 50% [**19**]. Graphene oxide with a $sp^3$ carbon configuration possessing low electrical conductivity was switched in an electric field in the $sp^2$ configuration of carbon, which led to high electrical conductivity. This process can be controlled both by adsorption/desorption of oxygen and by migration of oxygen-related groups.
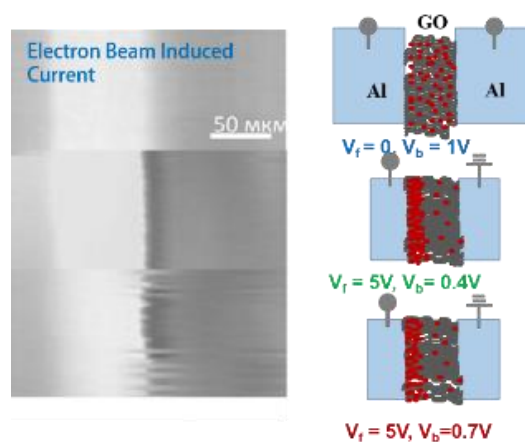


**Fig. 2.** Memristor based on Graphene/Graphene Oxide. Scanning electron microscope-remote electron beam induced current (REBIC) images of the Al/GO/Al structure with the modulation of the built-in potential barrier near the negatively biased Al electrode at different bias ($V_b$) and forming ($V_f$) voltages (left). $V_b$ = 1V; $V_f$ = 0V (REBIC) (left, top); $V_b$ = 0.4V; $V_f$ = 5V (REBIC) (left, middle); $V_b$ = 0.7V; $V_f$ = 5 V (REBIC) (left, bottom). A scale mark of 50 μm. The scheme of the Al/GO/Al structure at different bias ($V_b$) and forming ($V_f$) voltages (right). Red beads are oxygen-containing groups.

Recently, IBM announced a multi-level high-speed non-volatile memory based on graphene oxide [**20**]. A memory cell with a thickness of 8 nm and a size of 50 nm possessed a 4-level information storage (2-bit per cell) with a record and erase time of sub-5 ns, and also demonstrated excellent reliability and data storage capability.

Memory with the ability to store more than one bit per cell, that is, having multilevel memory states, is very attractive, since it offers a simple and economical way to increased memory capacity (e.g., modern CMOS NAND-Flash usually stores 2 or 3 bits per cell). Combining this capability with tiered storage with extremely high scalability is especially effective for implementing memory with ultrahigh storage volumes. Access to four very well-separated and stable memory states in nanoscale GO cells by monitoring the duration and amplitude of the write pulse was demonstrated [**20**]. Excitation pulses with amplitudes from 2 to 6 V and duration from 20 to 80 ns were used to determine the conditions for successful recording and erasing of multilevel memory states in Pt/GO/Ti/Pt and monitoring of the resulting cell resistance. The cells were completely switched from the RESET state, which can be considered as state 00 to memory states 01, 10 and 11 using pulses of −2.5 V/60 ns, −3.5 V/60 ns and − 4.5 V/60 ns respectively. Erasing of cells from 01, 10 and 11 states back to state 00 was successfully achieved for pulses +3 V/60 ns, +4 V/60 ns and +5 V/60 ns, respectively. A good separation of the levels of intermediate resistance has made it possible to provide a reliable reading process. Intermediate levels showed excellent reliability and were stable over time, both on rigid and flexible substrates. The reversible resistive switching observed in these devices was due to the migration of oxygen, which led to a change in the conductivity.

The photocatalytic oxidation of graphene coated with a layer of 10–15 nm ZnO nanoparticles under ultraviolet (UV) irradiation conditions led to the formation of self-organized G/GO memristors with very high density ($10^{12}$ cm$^{-2}$) [**12,16**]. **Fig. 3** shows the scheme of photocatalytic oxidation of graphene with ZnO nanoparticles and the electronic diagram of graphene/ZnO interface under UV irradiation. ZnO nanoparticles play a key role in the process of photooxidation of graphene. The bending of the bands upward in the ZnO nanoparticles is caused by a lower electron work function in ZnO (3.6 eV) compared to graphene (4.5 eV). Electron–hole pairs generated in ZnO (3.3 eV) under UV irradiation (reaction 1) are separated in a built-in electric field at the graphene/ZnO interface, which provides a hole flux (3.3 eV) to graphene. As a result, graphene is decorated with highly reactive hydroxyl radicals (·OH) through $O^{2-}$ and $H_2O_2$ (reactions 3–5) processes of photodecomposition of water molecules from moist air. Controlling the distribution of ZnO nanoparticles on graphene with a well reproducible size (~10 nm) makes it possible to create highly scalable nanoheterojunctions of G/GO for ultrahigh-density

memory (up to $10^{12}$ cm$^{-2}$ or 1 Tb on a chip for the vertical geometry of crossing electrodes, **Fig. 3c**). Memristors with a floating photogate are electrically read with or without optical excitation. The curve I-V of the graphene sample before oxidation demonstrates linear behavior and high conductivity of graphene (**Fig. 4 (a)**, black curve). The photocatalytic process leads to a decrease in current through the sample by two orders of magnitude and a nonlinear behavior indicating the formation of a bandgap in the oxidized graphene (**Fig. 4 (a)**, red curve). The rise in the temperature of moist air reduces the oxidation time of graphene. The G/GO heterostructures obtained by photocatalytic oxidation by blowing moist air at room temperature for 30 min and at 80°C for 5 min demonstrate a nonlinear behavior with a GO band width of about 3 eV, which reduces the conductivity of oxidized graphene by two orders of magnitude. The formed G/GO nanostructures demonstrated good photosensitivity to white light and photoresistive switching.
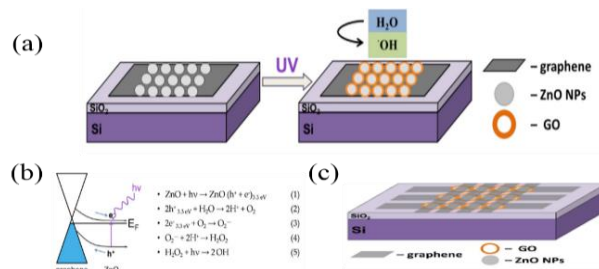


**Fig. 3.** (a) Scheme of photocatalytic oxidation of graphene coated with ZnO nanoparticles under UV light to form G/GO heterostructures on a Si/SiO$_2$ substrate, (b) Schematic electronic diagram of the G/ZnO interface under UV irradiation. Electron-hole pairs generated in ZnO (3.3 eV) under UV irradiation (reaction 1) are separated in a built-in electric field at the G/ZnO interface, providing a flux of holes to graphene, (c) Scheme of arrays of G/GO photomemristors in vertical geometry obtained by photocatalytic oxidation of graphene with ZnO nanoparticles.
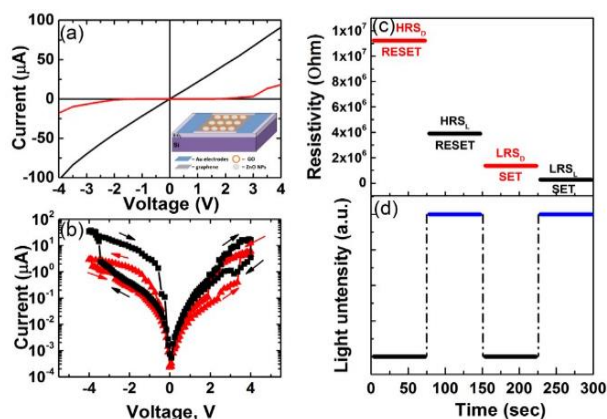


**Fig. 4.** (a) I-V characteristics of the 2–3 layer G/ZnO structure before (black) and after (red) photocatalytic oxidation in moist air for 30 min at room temperature. Insert-scheme for measuring the structure with lateral gold electrodes. (b) I-V characteristics for the G/GO nanostructure preliminarily polarized (+5 V, 15 min) with white light (black) and in the dark (red). (c) Resistive states of the G/GO photomemristor, which are switched by a voltage of −3.8/3.3 V (Reset/Set) in the dark and −3.5/4 V (Set/Reset) under white light pulses (d) and read at 2.5 V [**12**].

473

The photocurrent increased approximately six times at a bias voltage greater than 3 V. This indicates that the electron–hole pairs generated by light are effectively separated in the biased G/GO heterojunctions. **Fig. 4(b)** shows the I-V characteristics of the preformed G/GO nanostructure (+5 V, 15 min) when sweep voltage of −4 to 4 V under white light (black) and in the dark (red). Well reproducible bipolar hysteresis indicates a resistive switching of the structure with an on/off ratio of about 10 for 4 different resistive states HRSD, LRSD, LRSL and HRSL in the dark and light with switching voltages of −3.8/3.3 V (Reset/Set) and −3.5/4 V (Set/Reset), respectively (**Fig. 4(c)** and **(d)**). To form vertical memristive structures, ZnO nanorods (NR) grown on graphene can also be used **Fig. 5**. The vertical structure of the G/GO/ZnO nanorods (NR) allows selective excitation with UV light 380 nm. Resistive switching in heterostructures of G/GO/ZnO NR was observed at voltages <1 V with the ratio of high/low resistance $10^3$ after the forming process at 1 V [**18**]. The structure of resistive memory based on graphene and ZnO NR is promising for memristive devices with high density and low power consumption.

### Memristor with floating MoS$_2$ photogate

A memristor with a floating MoS$_2$ photogate polarized in an electric field under different lighting conditions demonstrates a multilevel switching [**13**]. **Fig. 6** shows the current–voltage curves (I-V) of the Au/MoS$_2$/Au structure (an inset in **Fig. 6(a)**) after polarization at 3 and 6 V. The nonlinear characteristics of a device with hysteresis indicate a memristive behavior. Furthermore, the memristor demonstrates a high photoresponse when illuminated with white light.

When the device is polarized at 3V, a smooth switching from HRSL3 to LRSL3 is observed under light illumination and from HRSD3 to LRSD3 in the dark with a ratio of on/off currents of about 2 and 4 at 1.2 V and 0.7 V, respectively (**Fig. 6(a)**). At a higher voltage (6 V), the device shows a sharp switching when excited by white light, from HRSL6 to LRSL6 at −2.9 V with an on/off ratio of about 10 and a smooth switching from HRSD6 to LRSD6 in the dark with an on/off ratio of about 3 at 0.7 V (the SET process of writing the ON state, **Fig. 6(b)**). When the applied voltage changes from 0 to positive voltage (4.2 V), the device returns to HRSL6 (RESET operation to clear the state ON to OFF). The memristive behavior of the device in darkness and in light is well reproduced up to 1000 cycles (**Fig. 6(c)** and **(d)**) and demonstrates the possibility of obtaining in the device a multilevel resistive switching and its control by means of an electric field in the dark and when excited by light. It should be noted that resistive switching controlled by the polarization of MoS$_2$ nanospheres is a faster process than ion transport, and the frequency of optical access is much higher than electrical addressing. A memristor polarized at 3V in darkness or in white light demonstrates four states that are read at a voltage of 0.7 V (HRSD3 and LRSD3) and 1.2 V (HRSL3 and LRSL3)

in the dark or in white light [**13**]. Polarization of the memristor at 6 V in darkness or under light leads to the formation of four more states that are read at a voltage of 0.7 V (HRSD6 and LRSD6) and 4 V (HRSL6 and LRSL6) in darkness or in light. These states are controlled electrically and optically, which is confirmed by the iterative operation of the memristor under various conditions of writing and reading [**13**]. Polarization of nanospheres in a photomemristor using an electric field and light pulses creates multilevel states. An analysis of the conductivity in these states of resistance shows that the polarization of nanospheres when excited by light leads to the formation of conductive paths. Reducing the gap between the electrodes can greatly minimize the operating voltage of the device.
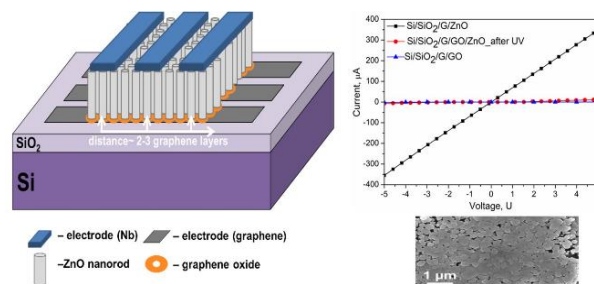


**Fig. 5.** Scheme of arrays of G/GO/ZnO NR photomemristors in vertical geometry (left) and a SEM image of the structure (lower right) with their current-voltage characteristics (upper right).
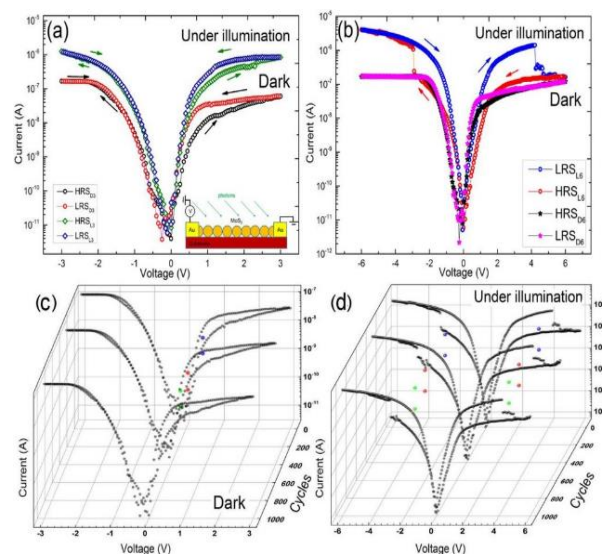


**Fig. 6.** Resistive switching of the nanospheric photomemristor Au/MoS2/Au. I-V characteristics in the dark or under white light (spectral maxima at 2.7 eV and 1.8 eV; device diagram on the inset in **Fig. 6(a)** with light excitation). The arrows on the curves indicate the direction of the voltage sweep; (a) I-V curves after 3V polarization. The device smoothly switches from HRSL3 to LRSL3 under light and from HRSD3 to LRSD3 in the dark with an on/off ratio of about 2 and 4 at 1.2 V and 0.7 V, respectively; (b) I-V curves after a 6 V voltage polarization. The device shows abrupt changeover of resistance when excited by light, from HRSL6 to LRSL6 at −9.2 V with an on/off ratio of about 10 and a smooth transition from HRSD6 to LRSD6 without light excitation with a switching factor on/off about 3 at 0.7 V. (c) Memristive characteristics of the device without excitation by light after several cycles. (d) Memristive characteristics of the device when excited by white light after several cycles [**13**].

Modulation of the barrier height at the boundaries of the nanospheres in an external electric field by light due to repolarization is a highly efficient process for high-speed signal processing. The memristor polarized at 3 V and 6 V has different states that can be electrically read at optical excitation in the form of four high-resistance states and four low-resistance states. The optical and electrical polarization of the memristor provides several nonlinear dynamic processes that allow us to build a system with a neuromorphic architecture, similar to a neural network.

## Conclusion

Memristive systems based on 2D-crystals, a new class of nonvolatile electronic components, which provides an opportunity for high-performance and low-energy computing and sensing. Self-assembled synapse-like graphene memristors controlled by transitions between $sp^3$ to $sp^2$ configurations of carbon under an electric field, can be used for interaction of electronic networks and neurons. 2D photomemristors with a floating photogate show multiple states controlled in a wide range of electromagnetic radiation and can find application for a wide range of tasks related to neuromorphic computations, image processing and recognition of sounds, movements and speech necessary to create artificial intelligence and for selective manipulation of neurons by light. The future development of 2D memristive systems should use the possibility of self-organizing technology to form artificial neural networks and heterointerface interactions of biocompatible 2D crystals with natural neurons.

## Acknowledgements

## Author's contributions

Conceived the plan: gnp, ook; Performed the expeirments: gnp, ook; Data analysis: gnp, ook; Wrote the paper: gnp, ook. Authors have no competing financial interests.

## References

1. Desai Sujay, B.; Madhvapathy Surabhi, R.; Sachid Angada, B.; Llinas Juan, Pablo; Wang Qingxiao; Ho Ahn, Geun; Pitner, Gregory; Kim Moon, J.; Bokor, Jeffrey; Hu, Chenming; Wong H.S. Philip; Javey Ali; *Science,* **2016**, *354,* 99.
2. Chua LO; *IEEE Transactions on Circuit Theory*, **1971**, *18,* 507.
3. Losev OV; *Telegraphy and Telephony without Wires, NRL.,* **1922**, *14,* 374.
4. Lossev O; *The Wireless World and Radio Review,* **1924**, *15,* 93.
5. Strukov, D.B.; Snider, G.S.; Stewart, D.R.; Williams, R.S.; *Nature,* **2008**, 453, 80.
6. Novoselov, K.S.; Geim, A.K.; Morozov, S.V.; Jiang, D.; Zhang, Y.; Dubonos, S.V.; Grigorieva, I.V.; Firsov, A.A.; *Science,* **2004**, *306,* 666.
7. Bendali, A; Hess, L.H; Seifert, M.; Forster , M.; Stephan, A.-F.; Garrido, J.A.; Picaud, S.A; *Adv. Healthcare Mater.* **2013**, *2*, 929.
8. Hess, L. H.; Jansen, M.; Maybeck, V.; Hauf, M.V.; Seifert, M.; Stutzmann, M.; Sharp, I.D.; Offenhäusser, A.; Garrido, J.A.; *Adv. Mater*, **2011**, *23*, 5045.
9. Hess Lucas, H.; Seifert, Max; Garrido, Jose A.; *Proceedings of the IEEE*, **2013**, *101,* 1780.
10. http://www.agenciasinc.es/Noticias/Desarrollan-protesis-de-retina-basadas-en-grafeno
11. Hébert, C.; Masvidal-Codina, E.; Suarez-Perez, A.; Calia A.B.; Piret, G.; Garcia-Cortadella, R.; Illa, X.; De la Cruz, J.M.D.; Casals, D.V.; Prats-Alfonso, E.; Bousquet Jessica; G., Philippe, G.; Yvert, B.; Villa, R.; Sanchez-Vives M.V.; Guimerà-Brunet, A.; Garrido J.A.; *Adv. Funct. Mater.*, **2017**, 1703976.
12. Kapitanova, O.O.; Panin, G.N.; Cho, H.D.; Baranov, A.N.; Kang, T.W.; *Nanotechnology.* **2017**, *28*, 204005.
13. Wang, W.; Panin, G.N.; Fu, X.; Zhang, L.; Ilanchezhiyan, P.; Pelenovich, V.O.; Fu, D.; Kang, T.W., *Scientific Reports*, **2016**, *6,* 31224.
14. Panin, G.N.; Kapitanova, O.O.; Lee, S.W.; Baranov, A.N.; Kang, T.W.; *Jap. J. Appl. Phys.,* **2011**, *50,* 070110.
15. Panin, G.N.; Kapitanova, O.O.; Lee, S.W.; Baranov, A.N.; Kang, T.W.; In Abstract of the 2nd Int. Symp. on Graphene Devices: Technology, Physics and Modeling. Sendai, Japan; **2010**.
16. Kapitanova, O.O.; Nanostructures with resistive switching based on graphene oxide [PhD thesis]. Moscow: Moscow State University; **2015**.
17. Kapitanova, O.O.; Panin, G.N.; Baranov, A.N.; Kang, T.W.; *J. Kor. Phys. Soc.*, **2012**, *60,* 1789.
18. Kapitanova, O.O.; Panin, G.N.; Kononenko, O.V.; Baranov, A.N.; Kang, T.W.; *J. Kor. Phys. Soc.,* **2014**, *64,* 1399.
19. Goldsmith, B.R.; Coroneus, J.G.; Khalap, V.R.; Kane, A.A.; Weiss, G.A.; Collins, P.G.; *Science.* **2007**, *315,* 77.
20. Nagareddy, V.K.; Barnes, M.D.; Zipoli, F.; Lai, K.T.; Alexeev, A.M.; Craciun, M.F.; Wright, C.D.; *ACS Nano,* **2017**, *11,* 3010.